Synthesis and Conformational Studies of Urobilin Difluoroboron Complexes. Unprecedented Solvent-Dependent Chiroptical Properties of the BF_2 Chelate of an Urobilinoid Analogue[1]

Albert Gossauer,*,† Felix Fehr,† Fredy Nydegger,† and Helen Stöckli-Evans‡

Contribution from the Institut für Organische Chemie der Universität, CH-1700 Fribourg, Switzerland, and the Institut de chimie de l'Université, CH-2000 Neuchâtel, Switzerland

Received June 3, 1996[⊗]

Abstract: Optically active difluoroboron complexes of both a conventional urobilin derivative (**3**) and a nonracemizable urobilin analogue (**4**) have been synthesized for the first time, and their structures have been determined, in solution, by means of $^1H\{^1H\}$NOE difference experiments. Whereas the BF_2 chelate **5** occurs in a "stretched" 9*Z*,4(5)-*ac*, 5(6)-*sc*,10(11)*sp*,14(15)-*sc*,15(16)-*ac* conformation in both dimethylformamide and methylene chloride solutions, the preferred conformation (**6** or **7**) of the difluoroboron complex of **4** is dependent on the solvent, thus giving rise to opposite CD curves in the aforementioned solvents. As revealed by X-ray diffraction analysis, however, only conformer **6** is present in the solid state, in which extended intermolecular hydrogen bonding involving the lactam groups takes place, independently of the solvent used for crystallization. Conformer **7**, on the contrary, is stabilized, in solution, by intramolecular NH···F bonds, as evidenced by measurements of "through-space" $^1H-^{19}F$ spin−spin coupling.

Introduction

Urobilinoids (urobilins and stercobilins) are the final products of heme catabolism in humans and other mammals.[2] This class of bile pigments deserve particular interest, however, since the existence of the urobilin chromophore has been demonstrated in both algal[3,4] and bacterial[5] accessory pigments of the phycoerythrin type, which are involved in the process of oxygenic photosynthesis in these organisms.

Within the scope of our work on the molecular origin of the unusual chiroptical properties of urobilinoids,[6] we have reported recently the synthesis of an optically active urobilin analogue (**4**)[7] in which methyl groups instead of H atoms are bound to the stereogenic centers of the bile pigment chromophore. Although the absolute configurations at the asymmetric C atoms of both this urobilin analogue and a conventional urobilin derivative (**3**)[6] have been established experimentally by X-ray diffraction analysis of derivatives of the corresponding 1,4,5, 10-tetrahydro-11*H*-dipyrrinones (**2** and **1b**, respectively), used as their synthetic precursors, the preferred (most likely helical) conformation of the optically active chromophores, in solution, cannot be inferred from these results. Therefore, any assignment of the actual helicity (P or M) of the urobilin chromophore is, until now, entirely reliant on the presumed relationship between absolute configuration at the stereogenic centers and the inherent dissymmetry of the dipyrrine chromophore within the molecule, as postulated by Moscowitz *et al.* more than 30 years ago.[8] Indeed, the reliability of this relationship is based on the assumption that intramolecular H-bonding is the determining factor for the stabilization of a particular conformer of the bile pigment molecule, a postulate which does not hold true for all kinds of substitution patterns of the urobilin molecule, as the present results reveal.

Results

In the course of the syntheses of urobilinoids **3** and **4**, we observed that the sign of the Cotton effect in the CD curves of their precursors, **1b** and **2,** respectively, is the same (*cf.* Figure 1), though the corresponding absolute configurations at C(4), as determined by X-ray diffraction analysis,[9] are opposite.[10] Most likely, the coincidence of sign of the CD curves reflects a similar relative spatial orientation of the α,*β*-unsaturated lactam and pyrrole chromophores in both tetrahydro-11*H*-dipyrrinones **1b** and **2**. As they mainly differ in the substituents on the lactam ring, the preferred conformation of the molecules

* To whom correspondence should be addressed. Phone: 41-26-300 8770. FAX: 41-26-300 9739. E-mail: albert.gossauer@unifr.ch.

† Université Fribourg.

‡ Université de Neuchâtel, Laboratoire de cristallographie chimique.

⊗ Abstract published in *Advance ACS Abstracts,* February 1, 1997.

(1) Part 19 in the series Syntheses of Bile Pigments. Part 18: Nesvadba, P.; Ngoc-Phan, D.; Nydegger, F.; Espinosa Ferao, A.; Gossauer, A. *Helv. Chim. Acta* **1994**, *77*, 1837.

(2) Watson, C. J.; Weimer, M.; Moscowitz, A.; Lightner, D. A.; Petryka, Z. J. Davis, E. *Biochem. Med.* **1969**, *2*, 484.

(3) Nagy, J. O.; Bishop, J. E.; Klotz, A. V.; Glazer, A. N.; Rapoport, H. *J. Biol. Chem.* **1985**, *260*, 4864.

(4) Killilea, S. D.; O'Carra, P. *Biochem. J.* **1985**, *226*, 723.

(5) Stadnichuk, I. N.; Romanova, N. I.; Selyakh, I. O. *Arch. Microbiol.* **1985**, *143*, 20.

(6) Pasquier, C.; Gossauer, A.; Keller, W.; Kratky, C. *Helv. Chim. Acta* **1987**, *70*, 2098 and references given therein.

(7) Floch, L.; Nydegger, F.; Gossauer, A.; Kratky, C. *Helv. Chim. Acta* **1994**, *77*, 445.

(8) Moscowitz, A.; Krueger, W. C. ; Kay, I. T.; Skaves, G.; Bruckenstein, S. *Proc. Natl. Acad. Sci. U.S.A.* **1964**, *52*, 1190.

(9) In our previous work,[6] partially resolved (+)-**1a** was transformed by reaction with (−)-(*S*)-1-(1-naphthyl)ethylamine into the corresponding *N*-[1-(1-naphthyl)ethyl]carboxamide, the absolute configuration of which at C(4) was determined by X-ray diffraction analysis to be *R*. Within the scope of the present work, enantiomerically pure carboxylic acid (−)-**1a** has been reacted with (+)-(*R*)-1-(1-naphthyl)ethylamine, yielding crystalline carboxamide **1c**. The X-ray structure analysis of the latter, which has been carried out in the laboratory of Professor Christoph Kratky (Institut für Physikalische Chemie der Universität Graz, Austria) has unequivocally established the absolute configuration at C(4) as *S*.

(10) A similar observation has been made with higher substituted 4-methyl-1,4,5,10-tetrahydro-11*H*-dipyrrinone derivatives (Spivey, A. C.; Caprettra, A.; Frampton, C. S.; Leeper, F. J.; Battersby A. R. *J. Chem. Soc., Perkin Trans. 1* **1966**, 2091). We thank Prof. A. Battersby for the communication of his results, prior to publication.

S0002-7863(96)01883-5 CCC: $14.00

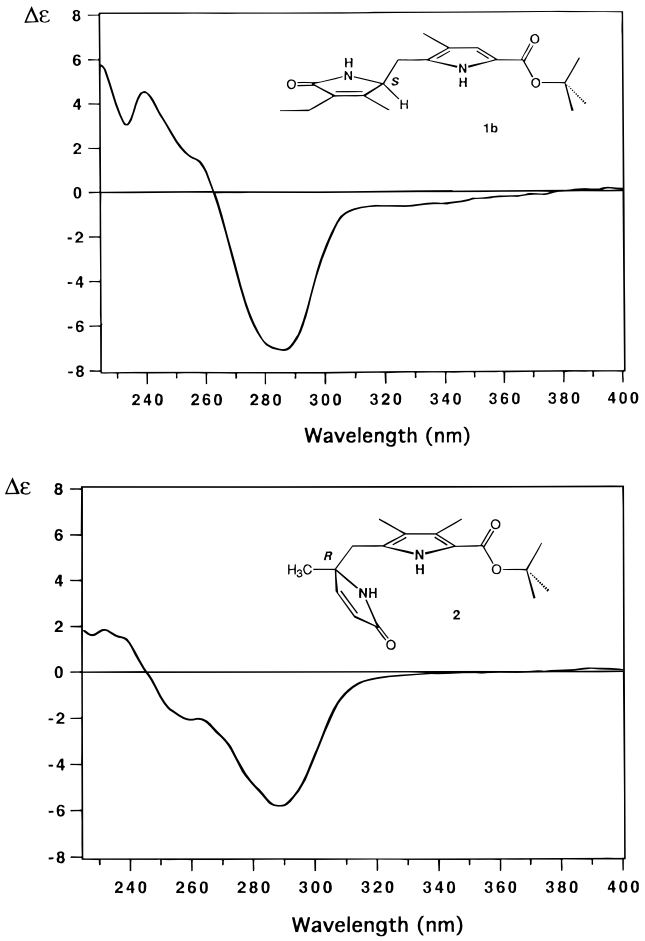

Figure 1. CD spectra of (−)-(4*S*)-**1b** and (−)-(4*R*)-**2**, both in MeOH (1.88×10^{-5} and 5.04×10^{-5} M, respectively).

is determined presumably in both cases by steric interactions of these substituents with the pyrrole moiety rather than by intramolecular hydrogen bonding. Moreover, as both dipyrrylmethanones **1b** and **2** represent partial structures of the corresponding urobilin derivatives synthesized therefrom, it is probable that similar interactions are also important in determining the conformation of these urobilinoids. In the latter, however, additional weak hydrogen bonds can be present between the lactam NH groups and the hydrogen-bridged dipyrrine chromophore,[8] and for this reason, the present conformational study has been carried out with the optical active difluoroboron chelates of urobilins **3** and **4** instead of the corresponding free bases or their protonated counterparts.

To our knowledge, difluoroboron chelates of urobilins have not been reported before in the literature. In the present work, they have been obtained by modifications of the procedure described for the preparation of the BF_2 complex of octaethylbiliverdin[11] (*cf.* Experimental Section). In contrast to the corresponding urobilin and its hydrochloride,[6] which are readily oxidised by air, solutions of difluoroboron chelate **5** in MeOH, $CHCl_3$, CH_2Cl_2, or dimethylformamide (DMF) may be kept for a long time without special precautions. In the presence of traces of acid, however, **5** decomposes within a few minutes.

In CH_2Cl_2 solution, the difluoroboron chelates of both urobilins **3** and **4** are strongly photoluminescent ($\Phi = 0.57$ and 0.48, respectively). It is worth mentioning that the circular polarization of the light emitted by both BF_2 chelates is fairly large. Particularly in the case of the BF_2 complex of **4**, the dissymmetry factor (g_{lum}),[12] measured in the peak of the luminescence band with a width of 6 nm, amounts to ($+0.94 \pm 0.1$) $\times 10^{-3}$, being equal to the dissymmetry factor in the absorption at the long-wavelength band ($\Delta\epsilon/\epsilon = +1.0 \times 10^{-3}$).[13] Molecular distortion upon excitation of the chromophore must therefore be small, in agreement with structure **7** of the complex, which is presumably stabilized by intramolecular NH···F bonding as implied by the NMR spectroscopic data discussed below.

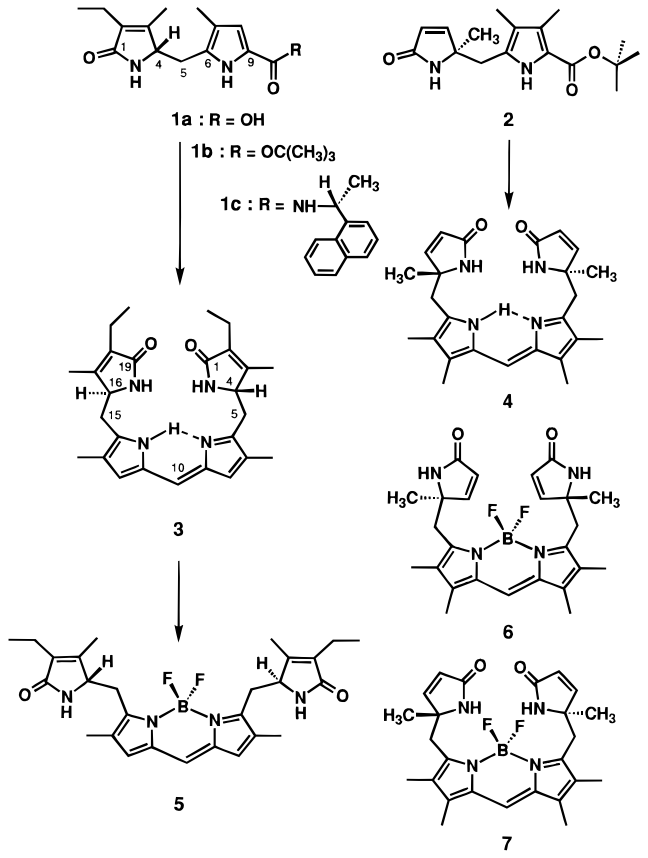

The structures of the BF_2 complexes of urobilins **3** and **4** have been established by spectroscopic data. A complete assignment of the ^{13}C-NMR signals of **5** (*cf.* Experimental Section) was achieved using the combination of ^{1}H{^{1}H} NOE difference spectroscopy, (^{13}C,^{1}H) shift correlated spectroscopy *via* long-range coupling with H−H decoupling (COLOC), and 2D heteronuclear (^{13}C,^{1}H) shift correlated spectroscopy (HETCOR).

Structure of the BF_2 Complex of 3. Both in dimethylformamide (DMF) and CH_2Cl_2 solution, the CD curves of the boron chelate **5** are negative (Figure 2). Within the temperature range from −20 to +50 °C, the sign of the Cotton effect remains unchanged (Figure 3). In the whole temperature range, the shape of the CD curves as well as λ_{max} (=546 ± 1 nm) of the Cotton effect are the same. The slight increment of $|\Delta\epsilon_{max}|$ at lower temperatures is probably due, in part, to the volume contraction of the solvent, and in part to the increase of the population of the preferred conformer. As the decrease of $|\Delta\epsilon_{max}|$ with rising temperature is linear, the change of entropy

(11) Bonfiglio, J. V.; Bonnett, R.; Buckley, D. G.; Hamzetash, D.; Hursthouse. M. B.; Abdul Malik, K. M.; McDonagh, A. F.; Trotter, J. *Tetrahedron* **1983**, *39*, 1865.

(12) Dekkers, H. P. J. M. See ref 32, pp 121−152.

(13) Private communication from Professor Harry P. J. M. Dekkers (Gorlaeus Laboratories, Department of Chemistry, The University of Leiden, The Netherlands). We are indebted to Professor Dekkers for measurements of the circular polarization of luminiscence of the difluoroboron chelates of urobilins **3** and **4**.

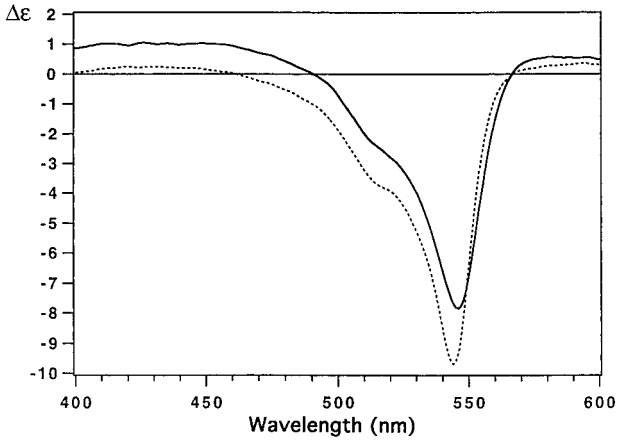

Figure 2. CD spectra of **5** in DMF (—) and in CH_2Cl_2 (- - -). Both 5.43×10^{-5} M.

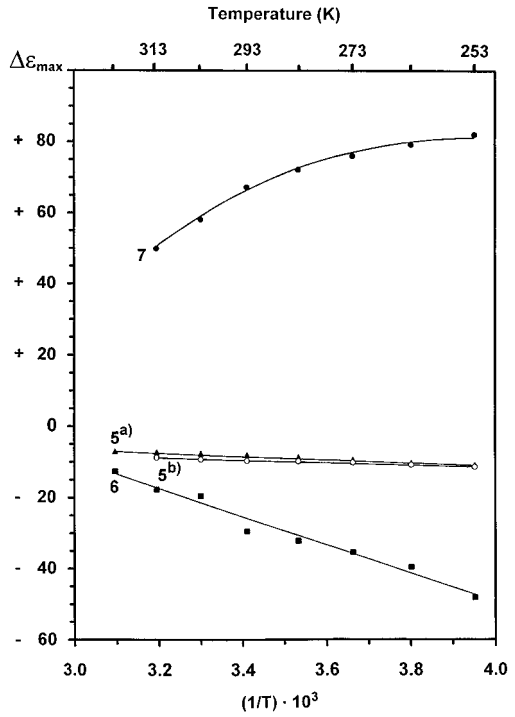

Figure 3. Dependence of $\Delta\epsilon_{max}$ of the BF_2 complexes **5** (a) in DMF (3.65×10^{-5} M) and (b) in CH_2Cl_2 (5.18×10^{-5} M), **6** (1.46×10^{-5} M), and **7** (1.32×10^{-5} M) on the temperature.

($\Delta S°$) of the mixture of conformers being at equilibrium must be negligible.[14] However, the presence of an equilibrium, in which conformations of different chiralities are nearly equally populated, as observed in the case of uncomplexed urobilins,[15] can be ruled out.

A conformational analysis of **5**, both in deuterated DMF and CD_2Cl_2 solution, was carried out by $^1H\{^1H\}$ NOE difference experiments (*cf.* Tables 1 and 2, respectively). Crucial for the interpretation of the experimental data is indeed the assignment of the resonance frequencies of the *pro-R* and *pro-S* hydrogen atoms at the methylene bridges. The following discussion is based on the choice of those of the two alternative assignments, which is in better agreement with the remaining NOE correlations determined in the same molecule. All quoted NOE correlations are assumed to be intramolecular.

(14) Legrand, M.; Rougier, M. J. Application of the optical activity to stereochemical determinations. In *Stereochemistry, Fundamentals and Methods*; Kagan, H. B., Ed.; Vol. 2, Thieme Verlag: Stuttgart, Germany, 1977; Vol. 2, pp 47−49.

(15) Lightner, D. A.; Docks, E. L.; Horwitz, J.; Moscowitz, A. *Proc. Natl. Acad. Sci. U.S.A.* **1970**, *67*, 1361.

Table 1. ^1H-NMR Signals of **5** (in DMF-d_7) Assigned by $^1H\{^1H\}$ NOE Difference Experiments

irradiated signal[a]		enhanced signal[a]	% enhancement
7.96[b]	(s, H-N(21), H-N(24))	2.11	1.7
		2.77	0.8
		4.45	4.7
7.61	(s, H-C(10))	7.08	15.0
7.08	(s, H-C(8), H-C(12))	2.11	3.6
		7.61	6.8
4.45	(dd, $J = 4.4, 9.7$, H-C(4), H-C(16))	1.99	2.9
		2.11	1.8
		3.44	5.0
		7.96	5.4
3.44	(dd, $J = 4.4, 13.4$, (*pro-R*)H-C(5), (*pro-R*)-H-C(15))	1.99	4.4
		2.77	20.1
		4.45	5.1
2.77	(dd, $J = 9.7, 13.4$, (*pro-S*)H-C(5), (*pro-S*)-H-C(15))	2.11	2.9
		3.44	9.8
		4.45	2.4
		7.96	1.2
2.23	(q, $J = 7.5$, CH_2-C(2), CH_2-C(18))	1.03	7.8
		1.99	1.4
2.11	(d, $J = 0.8$; *Me*-C(7), *Me*-C(13))	2.77	0.7
		4.45	0.7
		7.96	0.7
		7.08	2.3
1.99	(s, *Me*-C(3), *Me*-C(17))	2.23	0.4
		3.44	0.6
		4.45	1.0
1.03	(t, $J = 7.5$, *Me*-CH_2-C(2), *Me*-CH_2-C(18))	1.99	0.3
		2.23	2.8

[a] δ in ppm (360.14 MHz) referred to Me_4Si as internal standard, J in Hz. [b] At 298 K (chemical shift strongly dependent on temperature).

Table 2. ^1H-NMR Signals of **5** (in CD_2Cl_2) Assigned by $^1H\{^1H\}$ NOE Difference Experiments

irradiated signal[a]		enhanced signal[a]	% enhancement
7.08	(s, H-C(10))	6.86	9.2
6.86	(s, br, H-C(8), H-C(12))	2.07	3.1
		7.08	3.3
5.83[b]	(br, s, H-N(21), H-N(24))	2.07	1.6
		2.68	0.4
		4.38	5.7
4.38	(dd, $J = 3.8, 9.8$, H-C(4), H-C(16))	2.03	2.2
		2.07	1.2
		3.48	3.7
		5.83	3.5
3.48	(dd, $J = 3.8, 13.6$, (*pro-R*)H-C(5), (*pro-R*)-H-C(15))	2.03	5.4
		2.68	27.7
		4.38	6.3
2.68	(dd, $J = 9.8, 13.6$, (*pro-S*)H-C(5), (*pro-S*)-H-C(15))	2.07	3.5
		3.48	22.7
		4.38	1.9
		5.83	0.8
2.25	(q, $J = 7.6$, CH_2-C(2), CH_2-C(18)	1.06	7.2
		2.03	1.3
2.07	(d, $J = 1.0$, *Me*-C(7), *Me*-C(13))	2.68	0.9
		4.38	0.7
		5.83	0.5
2.03	(s, *Me*-C(3), *Me*-C(17))	2.25	0.6
		3.48	0.9
		4.38	1.0
1.06	(t, $J = 7.6$, *Me*-CH_2-C(2), *Me*-CH_2-C(18))	2.03	0.5
		2.25	2.8

[a] δ in ppm (360.14 MHz) referred to Me_4Si as internal standard, J in Hz. [b] At 298 K (chemical shift strongly dependent on temperature).

Thus, the lack of NOE between the *pro-R* hydrogen atoms of the CH_2 bridges and the H atoms bound to N suggests that

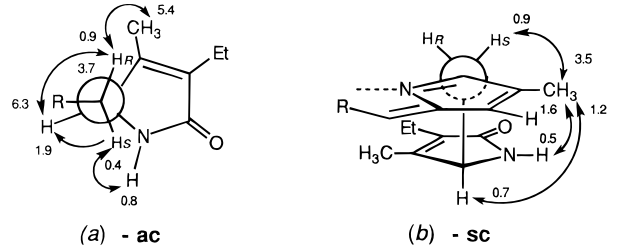

Figure 4. Newman projections along the axis of the (a) C(5)−C(4) and (b) C(6)−C(5) bonds of **5**, showing % enhancement (in CD_2Cl_2) of the $^1H\{^1H\}$ NOE correlations which are characteristic for the occurring conformation of the concerned bond. For the sake of clarity, the part of the molecule which is not taken into consideration is represented by *R*.

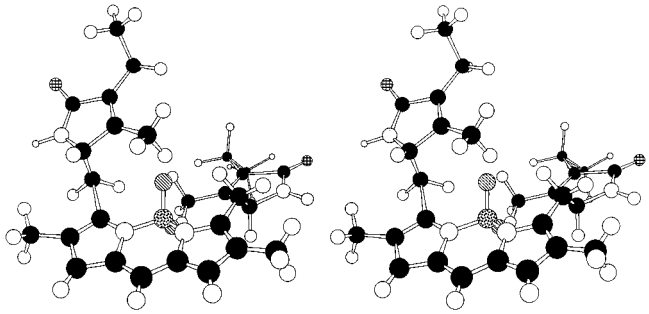

Figure 5. Stereoscopic representation of **5**.

they are located nearly *anti* to each other. Accordingly, whereas a reciprocal NOE between the corresponding *pro-S* H and H-N atoms is observed, irradiation at the resonance frequency of H_3C−C(3) and H_3C−C(17) enhances the intensity of the signal of the *pro-R* H atoms of the vicinal CH_2 bridges and *vice versa*, but not that of the *pro-S* H atoms. These NOE correlations are consistent with an −*ac* conformation[16] of the C(4)−C(5) and C(15)−C(16) bonds, which is further corroborated by the enhancement of intensity of the double doublet assigned to the protons on C(4) and C(16) upon irradiation of *both* hydrogen atoms at the adjacent methylene bridges (Figure 4a).

On the other hand, the observed reciprocal NOEs betweeen the H atoms bound to N and their neighboring H_3C−C(7) and H_3C−C(13) groups indicate that the N−H bonds of the terminal lactam rings of **5** point outward from the center of the molecule. As the singlet assigned to the methyl groups at C(7) and C(13) shows reciprocal NOEs only with the *pro-S* H atoms of the vicinal CH_2 bridges as well as with H−C(4) and H−C(16), respectively, the most likely conformation of the C(5)−C(6) and C(14)−C(15) bonds is −*sc*. (Figure 4b). Therefore, **5** occurs, both in DMF and CH_2Cl_2 solution, in a 9*Z*,4(5)-*ac*, 5(6)-*sc*,10(11)*sp*,14(15)-*sc*,15(16)-*ac* conformation (Figure 5).

BF_2 Complexes of 4. In contrast to **5**, the CD curves of the boron chelate of **4** are of opposite sign, when they are measured in DMF or in CH_2Cl_2 (Figure 6). The most straightforward interpretation of this phenomenon is a change of conformation of the bile pigment molecule, which is dependent on the solvent. Actually, in their study of the circular dichroism of urobilinoids, Lightner *et al.*[15] observed that in a 9:1 mixture of methanol and glycerol, as solvent, the population of some (possibly unfolded) conformers, in which the dipyrrine chromophore assumes the opposite chirality from that present in intramolecularly H-bonded molecules, increases at low temperatures. In the present case, however, the sign of the Cotton effect does not change, both in DMF and in CH_2Cl_2, on lowering the

(16) *sp* = syn-periplanar, *sc* = syn-clinal, *ac* = anti-clinal, and *ap* = anti-periplanar (*cf.* Klyne, W.; Prelog, V. *Experientia* **1960**, *16*, 521).

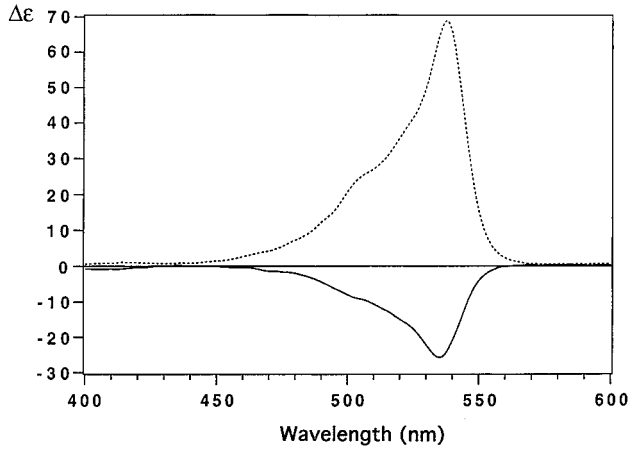

Figure 6. CD spectra of **6** in DMF (—) and **7** in CH_2Cl_2 (- - -) solution (1.14×10^{-5} and 1.20×10^{-5} M, respectively).

temperature from +50 to −20 °C (Figure 3). In the whole temperature range, the shape of the CD curves as well as λ_{max} of the Cotton effect in both DMF and CH_2Cl_2 is the same (535 ± 1 and 538 ± 1 nm, respectively). Therefore, the structure of the most abundant molecular species should remain unchanged, though its population apparently decreases when the temperature raises. Nevertheless, the temperature dependence of $|\Delta\epsilon_{max}|$ in both solvents is manifestly different. Thus, whereas the nearly linear decrease of $|\Delta\epsilon_{max}|$ on diminishing $1/T$, in DMF solutions, may be explained by a diminution of the population of the preferred conformer in favor of other conformers of comparable entropy,[14] the rate of decrease of $\Delta\epsilon_{max}$ in CH_2Cl_2 follows a binomial equation, which reflects a higher difference of entropy between the conformers (presumably **6** and **7**) being at equilibrium.

The reason for the striking contrast between the chiroptical properties of the boron chelates of **3** and **4** has to be sought probably in the presence of methyl groups at C(4) and C(16) of the latter, which render a extended conformation analogous to **5** less favorable because of steric repulsion between them and the methyl groups on C(7) and C(13), respectively. Apparently, the BF_2 complex of **4** can occur in two or more different conformations, which are stabilized either by intramolecular NH···F bonding in solvents of low polarity (*vide infra*) or by intermolecular H-bonding, in polar solvents. It is unclear, however, why no intramolecular NH···F bonding is operative in the BF_2 chelate of **3** in methylene chloride, as solvent.

As before, a conformational analysis of the BF_2 complex of **4**, both in DMF-d_7 and CD_2Cl_2 solution, was carried out by $^1H\{^1H\}$ NOE difference experiments (*cf.* Tables 3 and 4, respectively). Again, the assignment of the resonance frequencies of the *pro-R* and *pro-S* hydrogen atoms at the methylene bridges has been done on the basis of the best agreement with the remaining NOE correlations in the same molecule. The data reported below point out that the BF_2 chelate of **4** occurs in the conformations represented by **6** and **7** in DMF and methylene chloride, respectively.

Structure of the BF_2 Complex 6. In DMF-d_7 solution, reciprocal NOEs were found between the *pro-S* hydrogen atoms of the CH_2 bridges and the H atoms bound to N, as well as between the *pro-R* H (but not the *pro-S* H) and the hydrogen atoms on C(3) and C(17). Owing to the opposite absolute configuration at the stereogenic centers of **3** and **4**, however, the C(4)−C(5) and C(14)−C(15) bonds in the boron complex of the latter have the −*sc* instead of the −*ac* conformation (Figure 7a). Accordingly, irradiation of the methyl groups on C(4) and C(16) enhances the signals of *both* hydrogen atoms

Table 3. ^{1}H-NMR Signals of **6** (in DMF-d_7) Assigned by ^{1}H{^{1}H} NOE Difference Experiments

irradiated signal[a]		enhanced signal[a]	% enhancement
7.86[b]	(br. s, H-N(21), H-N(24))	3.36	1.9
		1.97	3.5
		1.50	2.8
7.67	(s, H-C(10)	2.18	17.1
7.31	(dd, J = 5.7, 1.5, H-C(3), H-C(17))	5.75	10.3
		3.47	0.8
5.75	(dd, J = 5.7, 1.5, H-C(2), H-C(18))	7.31	5.7
3.47	(d, J = 14.2, (*pro-R*)H-C(5), (*pro-R*)-H-C(15))	7.31	2.4
		3.36	20.7
		1.97	0.8
		1.50	1.5
3.36	(d, J = 14.2, (*pro-S*)H-C(5), (*pro-S*)-H-C(15))	7.86	2.5
		3.47	18.2
2.18	(s, *Me*-C(8), *Me*-C(12))	7.67	4.0
		1.97	1.4
1.97	(s, *Me*-C(7), *Me*-C(13))	7.86	1.0
		7.31	0.8
		3.47	0.6
		3.36	0.7
		2.18	2.3
1.50	(s, *Me*-C(4), *Me*-C(16))	7.86	1.5
		7.31	2.0
		3.47	1.0
		3.36	0.7

[a] δ in ppm (360.14 MHz) referred to Me_4Si as internal standard, J in Hz. [b] At 312 K (chemical shift strongly dependent on temperature).

Table 4. ^{1}H-NMR Signals of **7** (in CD_2Cl_2) Assigned by ^{1}H{^{1}H} NOE Difference Experiments

irradiated signal[a]		enhanced signal[a]	% enhancement
7.10	(s, H-C(10))	2.13	9.9
7.09	(dd, J = 5.7, 1.5, H-C(3), H-C(17))	5.81	5.7
		3.22	2.9
		1.85	4.9
		1.52	2.0
6.48[b]	(br. s, H-N(21), H-N(24))	3.47	1.5
		1.52	1.5
5.81	(dd, J = 5.7, 1.5, H-C(2), H-C(18)	7.09	4.7
3.47	(d, J = 14.2, (*pro-S*)H-C(5), (*pro-S*)-H-C(15))	6.48	2.4
		3.22	41.2
		1.52	3.7
3.22	(d, J = 14.2, (*pro-R*) H-C(5), (*pro-R*)-H-C(15))	7.09	6.0
		3.47	39.0
		1.85	5.3
		1.52	2.8
2.13	(s, *Me*-C(8), *Me*-C(12))	7.10	2.8
		1.85	1.6
1.85	(s, *Me*-C(7), *Me*-C(13))	7.09	1.2
		3.22	0.8
		2.13	1.6
1.52	(s, *Me*-C(4), *Me*-C(16))	7.09	1.6
		6.48	1.0
		3.47	1.3
		3.22	0.6

[a] δ in ppm (360.14 MHz) referred to Me_4Si as internal standard, J in Hz. [b] At 298 K (chemical shift strongly dependent on temperature).

at the adjacent methylene bridges, as it may be expected for a staggered conformation in which these methyl groups are situated between *pro-R* H and *pro-S* H.

The conformation of the C(5)−C(6) and C(14)−C(15) bonds was deduced from the reciprocal NOEs between the methyl groups at C(7) and C(13) and the H atoms bound to N, which suggest that the N−H bonds of the terminal lactam rings of **6**, as in the case of **5**, point outward from the center of the molecule. However, as evidenced by the reciprocal NOE between H_3C−C(7) and H_3C−C(13) and the *pro-R* H atoms at the vicinal methylene bridges, which is absent in the ^{1}H-NMR spectrum of **5**, the preferred conformation of the C(5)−C(6) and C(15)−C(16) bonds is different in both difluoroboron chelates (Figure 7b). Thus, the 9*Z*,4(5)-*sc*,5(6)-*sp*,10(11)*sp*, 14(15)-*sp*,15(16)-*sc* conformation is in best agreement with the NOE difference spectra of **6** in DMF-d_7.

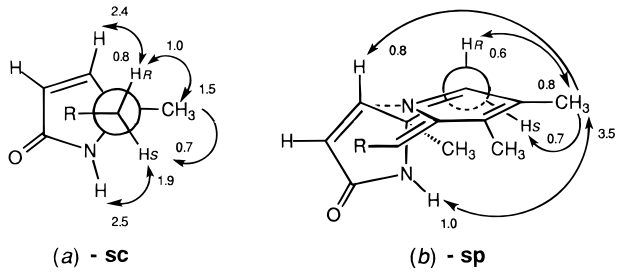

Figure 7. Newman projections along the axis of the (a) C(5)−C(4) and (b) C(6)−C(5) bonds of **6**, showing % enhancement of the ^{1}H-{^{1}H} NOE correlations which are characteristic for the occurring conformation of the concerned bond. For the sake of clarity, the part of the molecule which is not taken into consideration is represented by *R*.

The above assignment could be confirmed by X-ray diffraction analysis of a crystalline sample,[17] which was obtained from a solution of the BF_2 complex of **4** in DMF by diffusion of diethyl ether vapor (Figure 8). In the crystal, symmetry-related molecules are H-bonded *via* the O atom of the carbonyl group and the H atom of the lactam group, thus linking the molecules to form a two-dimensional sheet extending in the *bc* plane (Figure 9).

Structure of the BF_2 Complex 7. As mentioned above, the molecule of the difluoroboron chelate of **4** has a different shape when methylene chloride is used, as a solvent. The assignment of the resonance frequencies of the *pro-R* and *pro-S* hydrogen atoms at the methylene bridges has been done, as in the precedent cases, on the basis of the best agreement with the

(17) A crystal specimen of 0.38 × 0.19 × 0.19 mm^3 was investigated at 223(3) K on a Stoe AED2 four-circle diffractometer with monochromatic MoKα radiation (λ = 0.710 73 Å) using 2Θ/ω scans in the 2Θ range 4−45°. Crystal cell parameters were determined from the ±ω values of 10 reflections and their equivalents in the range 18° < 2Θ < 23.6°: orthorhombic, space group $C222_1$, with cell dimensions a = 16.536(9) Å, b = 23.863(14) Å, c = 7.159(4) Å, $\alpha = \beta = \gamma$ = 90°, V = 2825(3) Å^3, Z = 4 for $C_{25}H_{29}BF_2N_4O_2$, density (calcd excluding the disordered solvent molecule, see below) = 1.096 g/cm^3, F(000) = 984. The crystal diffracted very poorly, only 516 of the 1083 collected reflections could be considered to be independent ($I_{obs} > 2\sigma(I)$). The structure was solved by direct methods using the program SHELXS86 (Sheldrick, G. M. SHELXS86. *Acta Crystallogr., Sect. A* **1990**, *A46*, 467). The refinement and all further calculations were carried out using SHELXL93 (Sheldrick, G. M. SHELXL93. A program for crystal structure refinement. University of Göttingen, Germany, 1993). The H atoms were included in calculated positions as riding atoms. The non-H atoms were refined anisotropically, using weighted full-matrix least-squares on F^2. In the final difference maps a small amount of residual density was located at a position situated centrally between atoms C(13) and C(13′). It was assumed to be due to a highly disordered molecules of the solvent (DMF), used for recrystallization. CACL SQUEEZE routine, in the program PLATON (Spek, A. L.; PLATON. *Acta Crystallogr., Sect. A*, **1990**, *A46*, C-34), was used to modify the *hkl* file to remove this electron density. Refinement was continued and resulted in a final R_1 = 0.095 and R_w = 0.171 for 516 observed reflections. Two atoms, C(2) and C(3), were however, nonpositive definite, due to the very reduced number of observed reflections per parameter (516/159). The molecule possesses a crystallographic C_2 axis, on which the C(10) and B(1) atoms are located. The bond lengths and angles are normal, within experimental error. The numbering scheme used is apparent from Figure 7, which was drawn using the program XTAL-GX (Hall, S., Boulya du B., Eds. *Xtal-GX*; University of Western Australia, 1995). Full tables of atomic parameters and bond lengths and angles may be obtained from the Cambridge Crystallographic Data Centre, U.K., on quoting the full journal citation. Further details may be obtained from the author (H.S.-E.).

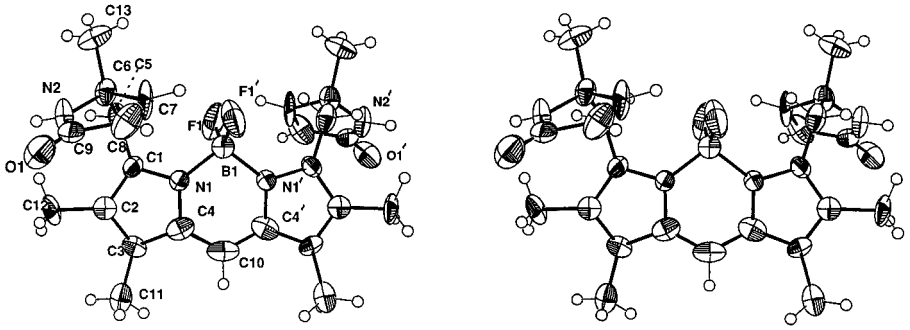

Figure 8. Stereoview of the molecular structure of **6**. Anisotropic atomic displacements ellipsoids, as drawn by ORTEP, represent the 50% probability surfaces.

remaining NOE correlations in the same molecule. Moreover, the dependence of the chemical shifts of both H atoms on the solvent used could be followed by adding increasing amounts of DMF-d_7 to the solution of the chelate in CD_2Cl_2, so that the assignments in the latter solvent are consistent with those made before for **6** (Figure 10).

In CD_2Cl_2 solution, the NOEs around the C(4)−C(5) and C(15)−C(16) bonds of the difluoroboron chelate of **4** correspond to those observed in DMF-d_7 solution (*cf.* Tables 3 and 4). Therefore, the same staggered conformation (−*sc*), in which the methyl groups on C(4) and C(16) are situated between *pro-R* H and *pro-S* H has to be assumed (Figure 11a).

On the other hand, both of the signals assigned to H−C(3) and H−C(17) and the doublet assigned to the *pro-R* hydrogen atoms at the CH_2 bridges become stronger upon irradiation at the resonance frequency of H_3C−C(7) and H_3C−C(13). Both NOEs are reciprocal (Figure 11b). As a +*sc* conformation of the C(5)−C(6) and C(14)−C(15) bonds is compatible with these correlations, the BF_2 complex of **4** probably occurs, in methylene chloride as solvent, in a circular 9*Z*,4(5)-*sc*,5(6)+*sc*,10(11)*sp*, 14(15)+*sc*,15(16)-*sc* conformation **7** (*cf.* Figure 12).

The suspicion that such a conformation may be stabilized by intramolecular NH···F bonding was verified by measuring the "through-space" coupling[18] between the H atoms bound to nitrogen in the lactam rings and the fluorine atoms bound to boron. "Through-space" nuclear spin−spin coupling *via* nonbonded interactions between fluorine and different nuclei has been observed mainly in rigid aromatic compounds, in which the distance between the interacting atoms is determined by the constitution of the molecule.[19] In such systems, "through-space" $^1H-^{19}F$ coupling arises from interactions of lone-pair orbitals on the fluorine atom with filled σ and π orbitals on the carbon atom to which the coupled hydrogen atom is bonded rather than from direct interactions between the fluorine atom and the hydrogen atom.[20] To the best of our knowledge, however, neither "through-space" $^1H-^{19}F$ coupling between fluorine atoms and hydrogen atoms bonded to *nitrogen* has been reported hitherto in the literature nor a dependence of the coupling constant on conformational changes of the geometry of the molecule, other than restricted rotation on one single bond[21] has been determined in these studies.

In the ^{19}F-NMR spectrum of each of the BF_2 chelates **5**−**7**, a quartet is visible, which arises from $^{11}B-^{19}F$ spin−spin coupling. Some overlapping of the bases of these signals results from additional peaks of low intensity due to coupling of the nuclear spin of the ^{19}F atoms with that of the less abundant

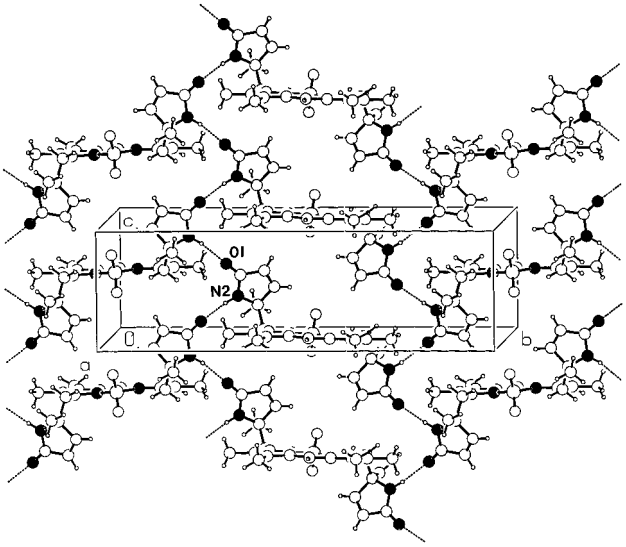

Figure 9. Crystal structure of **6**. Intermolecular hydrogen bonds are represented by dashed lines: [N2−H2···O1^a, H2···O1^a, 2.049(13) Å], [N2···O1^a, 2.844(13) Å], [N2−H2···O1^a, 151.6(4)°]; *a*: 0.5 − *x*, 0.5 − *y*, *z* − 0.5.

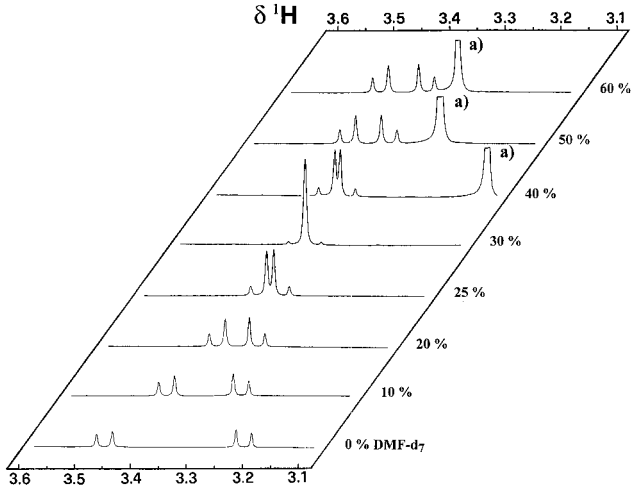

Figure 10. ^1H chemical shifts (500.13 MHz, δ in ppm referred to Me_4Si as internal standard) of the H atoms at the methylene bridges of the BF_2 chelate of **4** in dependence of the DMF-d_7 content in CD_2Cl_2 solutions. Samples are all 2.6×10^{-3} M. The crossing-over of the signal positions corresponding to the *pro-R* and *pro-S* H atoms suggests a solvent-dependent equilibrium between to conformations in which the environments of both protons are mutually exchanged (*cf.* Figures 6 and 9). (a) absorption due to the H_2O contained in DMF-d_7.

(18) Mallory, F. B.; Mallory, C. W.; Ricker, W. M. *J. Org. Chem.* **1985**, *50*, 457 and references cited therein.

(19) Berger, S.; Braun, S.; Kalinowski, H.-O. *NMR-Spektroskopie von Nichtmetallen*; ^{19}F-NMR-Spektroskopie; Georg Thieme Verlag: Stuttgart, Germany, 1994; Vol. 4, pp 148−153.

(20) Mallory, F. B.; Mallory, C. W.; Ricker, W. M. *J. Am. Chem. Soc.* **1975**, *97*, 4770.

(21) (a) Yamamoto, G.; Oki, M. *J. Org. Chem.* **1984**, *49*, 1913. (b) Yamamoto, G.; Oki, M. *Tetrahedron Lett.* **1985**, *26*, 457. (c) Mallory, F. B.; Mallory, C. W. *J. Am. Chem. Soc.* **1985**, *107*, 4816.

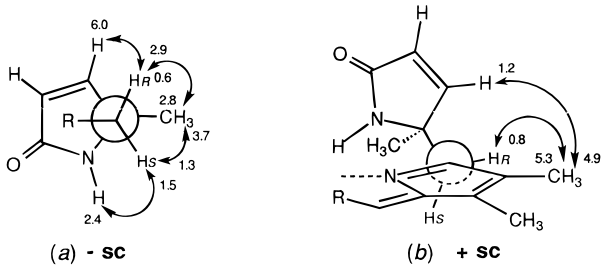

Figure 11. Newman projections along the axis of the (a) C(5)−C(4) and (b) C(6)−C(5) bonds of **7**, showing % enhancement of the ^{1}H-{^{1}H} NOE correlations which are characteristic for the occurring conformation of the concerned bond. For the sake of clarity, the part of the molecule which is not taken into consideration is represented by *R*.

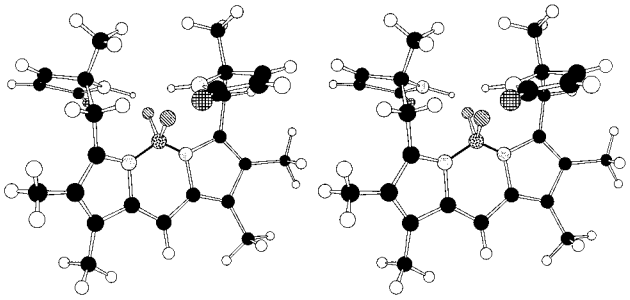

Figure 12. Stereoscopic representation of **7**.

(19.6%) ^{10}B isotope. Upon irradiation at the resonance frequency of the boron atom, the decoupled spectra show each a singlet in the range between δ = 10.8 and 18.4 ppm (*cf.* Experimental Section). In the spectrum of **7**, however, the singlet is perceptively broader ($\Delta\nu_{1/2} \approx 20$ Hz) than all the others, probably due to "through-space" ^{1}H−^{19}F coupling between the fluorine atoms and the hydrogen atoms of the CONH groups. This was confirmed by the ^{1}H-NMR spectrum of the BF_2 chelates **5**−**7** in the range of absorption of the protons bound to nitrogen (Figure 13). Actually, the shape of the resonance signal assigned to these protons is perceptively different in the case of **7** (Figure 13d, on the left) to that of the BF_2 chelates **5** and **6**. In the dispersion mode, the spectrum of **7** shows a manifest splitting of the resonance signal of the protons at δ 6.46, from which a "through-space" ^{1}H−^{19}F coupling constant of 4.6 Hz can be determined (Figure 13d, on the right). Upon inverse gated ^{19}F GARP decoupling,[22] the doublets collapse to a single dispersion curve (Figure 13e, on the right) similar to that observed in the spectra of **5**, both in DMF-d_7 and CD_2Cl_2 (Figure 13, parts a and b, respectively), as well as in the spectrum of the BF_2 complex of **4**, when measured in DMF-d_7 (Figure 13c).

After our attempts to obtain crystals of the BF_2 complex **7** in a quality suitable for X-ray diffraction studies became also successful, we expected to be able to confirm the structure assigned before by spectroscopic methods. Surprisingly, however, the X-ray diffraction analysis of the crystals obtained by diffusion of *n*-hexane vapor into a solution of the BF_2 chelate of **4** in $CHCl_3$[23] revealed a C_2-symmetric molecular structure, which is identical to that found for **6**.[24] Although it is well-known that flexible molecules may adopt different conformations in solution and in the crystal, the above results emphasize that the structure, and hence the chiroptical properties of chiral bile pigments, cannot be inferred from their structure in the solid state.

Discussion

It becomes clear from the above results that the relationship between the absolute configuration of the urobilinoid chromophore and the sign of the corresponding Cotton effect curve depends on the conformation of the molecule as a whole rather than on the absolute configuration of the stereogenic centers. It must be pointed out, however, that whereas the optical activity of urobilins, both in their free and protonated forms, is explained in terms of a displacement of the equilibrium between two mutually interconvertible inherently dissymmetric dipyrrine chromophores toward the M or P enantiomer caused by intramolecular hydrogen bonds with the vicinal stereogenic moieties of the molecule, the optical activity of the corresponding, essentially planar difluoroboron chelates should be rather a consequence of a "chiral perturbation" of the inherently achiral boron complexing dipyrrine chromophore produced by the adjacent lactam rings. The nature of this "chiral perturbation" may be similar to that observed in chiral β,γ-unsaturated ketones, in which the interaction between two inherently achiral chromophores present in the same molecule suffices to generate the high rotational strength which is characteristic for inherently chiral chromophores.[25]

Indeed, the notion of an inherently achiral moiety in a chiral molecule is only a fiction,[26] a differentiation between inherently achiral and inherently chiral chromophores is based on the observation that the latter usually produce strong Cotton effects, whereas inherently achiral transitions tend to have low rotational strengths. In the bile pigment series, strong Cotton effects may be displayed by derivatives devoid of stereogenic centers, when certain chiral conformations become stabilized. A typical example is the protobiliverdin IXγ chromophore, which occurs in the cabbage butterfly (*Pieris brassicae* L.) bound to an apoprotein. The latter stabilizes a helical conformation of the bile pigment molecule in the P configuration, giving rise to a CD Cotton effect in the visible range close to $\Delta\epsilon_{max} = 100$.[27] When bound to human serum albumin, bilirubin, on the other hand, displays extremely solvent-dependent Cotton effects,[28] which result from excited state induced electric dipole−dipole interaction between the two proximal dipyrrinone chromophores (*cf.* ref 29). Intramolecular exciton coupling between the electric transition moments of the boron-complexing dipyrrine chromophore and the pyrrolinone chromophore of the BF_2 chelates **5**−**7**, however, seems to be unlikely because of the large separation of the absorption maxima (λ_{max}= 528[30] and 210 nm,[31] respectively) of both chromophores (*cf.* ref 32).

(22) GARP = globally optimized alternating-phase rectangular pulses (*cf.* Shaka, A. J.; Barker, P. B.; Freeman, R. *J. Magn. Reson.* **1985**, *64*, 547).

(23) In our hands, the quality of the crystals obtained from CH_2Cl_2 solutions was insufficient for X-ray diffraction analysis. Nevertheless, the CD spectra of **7** in CH_2Cl_2 and $CHCl_3$ are identical.

(24) Gossauer, A.; Nydegger, F.; Schmidt, A.; Kratky, C. Manuscript in preparation.

(25) (a) Moscowitz, A.; Mislow, K.; Glass, M. A. W.; Djerassi, C. *J. Am. Chem. Soc.* **1962**, *84*, 1945. (b) Schippers, P. H.; Dekkers, H. P. J. M. *J. Am. Chem. Soc.* **1983**, *105*, 79.

(26) Deutsche, C. W.; Lightner, D. A.; Woody, R. W.; Moscowitz, A. *Ann. Rev. Phys. Chem.* **1969**, *20*, 407−448.

(27) Huber, R.; Schneider, M.; Mayr, I.; Müller, R.; Deutzmann, R.; Suter, F.; Zuber, H.; Falk, H.; Kayser, H. *J. Mol. Biol.* **1987**, *198*, 499.

(28) Pu, Y.-M.; McDonagh, A. F.; Lightner, D. A. *J. Am. Chem. Soc.* **1993**, *115*, 377.

(29) Person, R. V.; Peterson, B. R.; Lightner, D. A. *J. Am. Chem. Soc.* **1994**, *116*, 42.

(30) Vos de Wael, E.; Pardoen, J. A.; van Koeveringe, J. A.; Lugtenburg, *J. Recl. Trav. Chim. Pays-Bas* **1977**, *96*, 306.

(31) Bordner, J.; Rapoport, H. *J. Org. Chem.* **1965**, *30*, 3824.

(32) Nakanishi, K.; Berova, N. In *Circular Dichroism: Principles and Applications*; Nakanishi, K., Berova, N., Woody, R. W., Eds.; VCH Publ., Inc.: New York, 1994; pp 361−398.

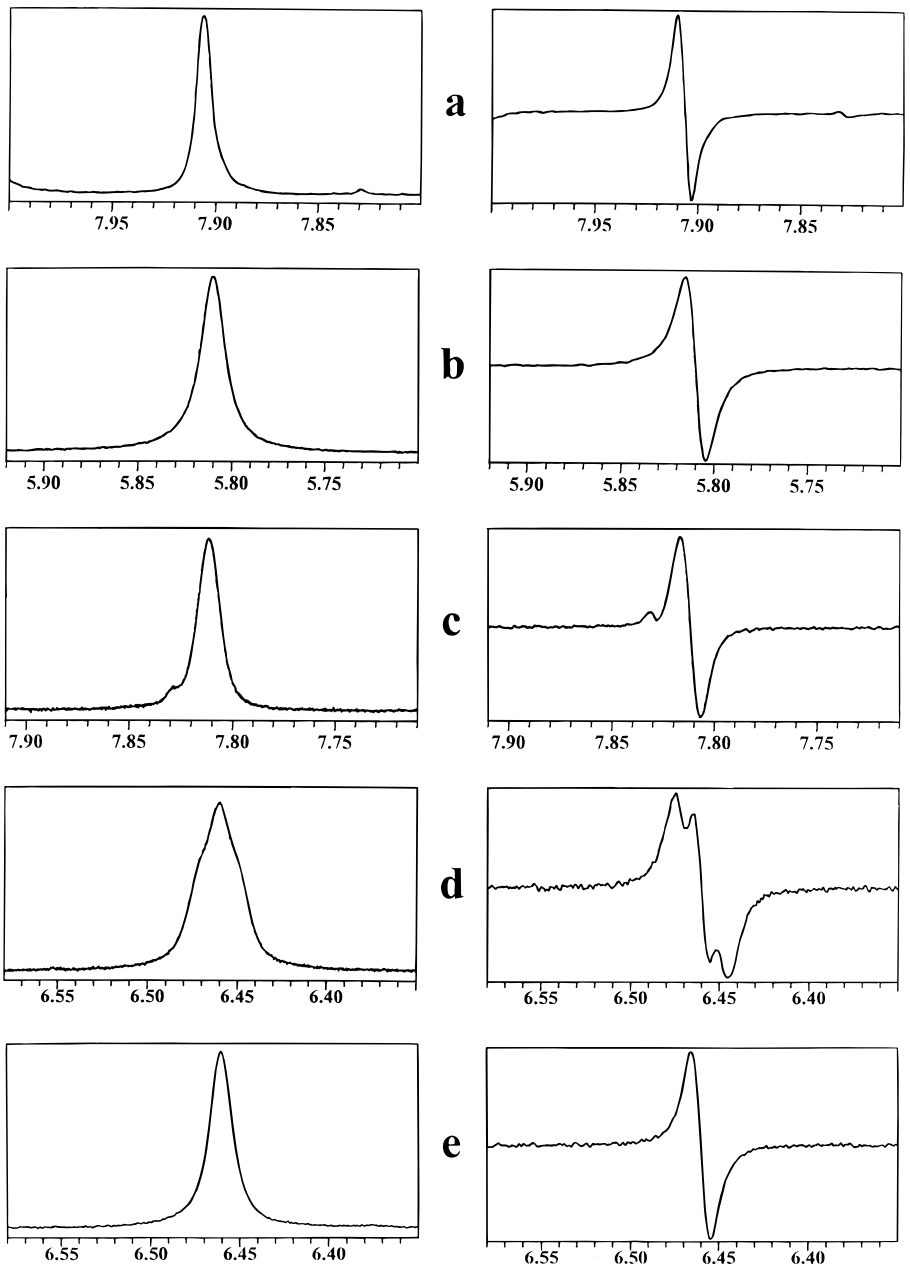

Figure 13. (left) ^{1}H-NMR absorption bands (500.13 MHz, δ in ppm referred to Me_4Si as internal standard) of the H atoms bound to N in the BF_2 chelates **5** [(a) in DMF-d_7 and (b) in CD_2Cl_2], **6** [(c) in DMF-d_7], and **7** [(d) in CD_2Cl_2]. (e) Same as d after ^{19}F-decoupling. (right) First derivatives of the same curves.

In the present case, the circular dichroism ($\Delta\epsilon_{538} = +67$) measured for the difluoroboron complex **7**, in CH_2Cl_2 as solvent, equals that of the protonated ligand ($\Delta\epsilon_{496} = +69$), its D-line specific rotation is even higher ($[\alpha]^{20}_D = +9700°$ *vs* $+4900°$) (*cf.* ref 7). When measured in DMF, both the circular dichroism ($\Delta\epsilon_{535} = -29$) and the specific rotation ($[\alpha]^{20}_D = -3900°$) of **6** are significantly lower than those of **7**, probably because of the more rigid structure of the latter, which is stabilized by intramolecular NH···F bonding, as discussed above. Interestingly, both the circular dichroism and the D-line specific rotation of **6** are higher than those of the corresponding urobilin complex **5**. Actually, both the circular dichroism ($\Delta\epsilon_{546} \approx -10$) and optical activity ($[\alpha]^{20}_D = -2940°$) of the latter are lower than those of the corresponding (presumably helical-shaped) hydrochloride[6] ($\Delta\epsilon_{499} \approx -53$ and $[\alpha]^{20}_D = -5000°$).

These results are difficult to explain in terms of a spring-washer-like deformation of the boron complexing dipyrrine chromophore, since the latter, as evidenced by the X-ray diffraction analysis of **6** is planar (*cf.* Figure 8). Thus, according to the postulate of an inherent dissymmetric dipyrrine chromophore, the skewing of the latter in **7** should be approximately the same as in the hydrochloride of **4** (*vide supra*). Even taking into account the contribution of intramolecular NH···F bonding in **7**, such a deformation is highly unlikely. As mentioned before, the origin of the high rotational strengths of difluoroboron chelates **5**−**7** may be rather a consequence of a "chiral perturbation" similar to that observed in chiral β,γ-unsaturated ketones, for which a quantitative chirality rule is available.[25b]

Empirically, the chiroptic data of the difluoroboron chelates described in the present work are consistent with a model representation, in which the dipyrrine chromophore is oriented horizontally and its C_2-symmetry axis as well as the nitrogen atoms are directed toward the observer. In this way, the electric dipole transition moment of the main absorption band in the visible range of the dipyrrine BF_2 chelate chromophore, the direction of which has been determined by means of the liquid-

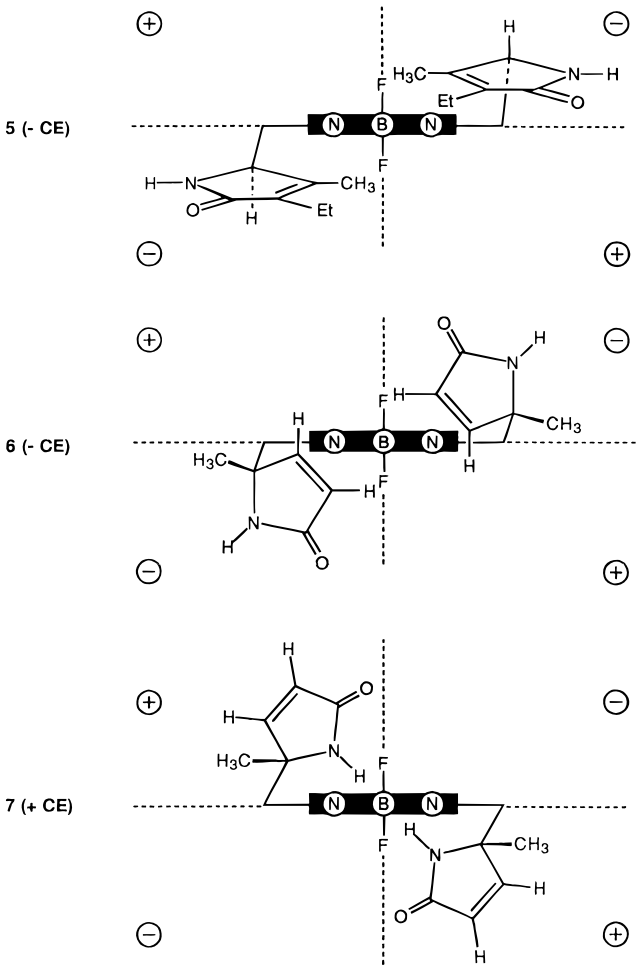

Figure 14. Empirical correlation between the preferred conformations of urobilin difluoroboron complexes **5**−**7** with the sign of their corresponding Cotton effect curves. View along the C_2-symmetry axis of the dipyrrine chromophore (represented by a bold bar).

crystal-induced circular dichroism technique,[33] lies transversely oriented with respect to the observer. The sign of the Cotton effect is determined by the occupation of the quadrants defined by the intersecting symmetry planes of the isolated dipyrrine chromophore (*cf.* ref 34). Thus, according to the projections depicted on Figure 14, both BF_2 chelates **5** and **6** should display CD curves of the same sign, whereas in the case of complex **7**, the sign should be opposite. This prediction is in agreement with the experimental data, whereby the substituent effects are consignate[35] with respect to the location of the lactam rings in the quadrants of the reference system defined above. Moreover, it must be pointed out that according to the molecular geometry established above for the urobilin BF_2 chelates, which have been investigated in the present work, the lactam rings of conformers **6** and **7** lie closer to the dipyrrine chromophore than those of conformer **5**, thus explaining the relative low rotational strength of the latter.

Consequently, the location of the substituents of the dipyrrine chromophore in the reference system and not the absolute configuration of the stereogenic centers in the molecule seems to be critical in determining the sign of the Cotton effect. As a matter of fact, the BF_2 chelates of urobilinoids **4** and **5** display, when measured in DMF, Cotton effects of the same sign, although their configurations at the stereogenic atoms C(4) and C(16) are opposite. Indeed, as evidenced by NOE difference spectroscopy, the conformations of both molecules are different. On the other hand, in CH_2Cl_2 as solvent, both the hydrochloride of **3**, the preferred conformation of which is thought to be helical[6] and, therefore, similar to that of the boron complex **7** and the latter, display Cotton effects of opposite signs according to their opposite configurations at the stereogenic centers.

In order to confirm the above results, the synthesis of a series of different urobilinoids and their BF_2 chelates as well as the elaboration of a theoretical model capable of correlating the geometry of urobilinoid molecules with experimental determined CD data is, at present, in progress.

Conclusions

The above results emphasize the inherent difficulty in assigning molecular structures on the basis of chiroptical data, when dealing with conformationally flexible systems. The present work leads to following conclusions:

(i) In the urobilinoid series, high specific rotations (up to $[\alpha]^{20}_D = +9700$) can be attained even in the absence of an inherently dissymmetric chromophore.

(ii) An unequivocal relationship between the absolute configuration at the stereogenic centers of urobilinoids and the sign of the corresponding Cotton effect curves cannot be established in general, but only for a particular conformation of the molecule.

(iii) Although for the first time the molecular structure of an optical active urobilinoid has been determined by X-ray diffraction analysis, the chiroptical properties of the individual molecules cannot be inferred, in general, from their structure in the solid state.

Experimental Section

Materials. Solvents for chemical reactions and chromatography were generally dried and distilled prior to use. All air- and water-sensitive reactions were carried out under Ar. Reactions were monitored by thin-layer chromatography (TLC) on E. Merck silica gel $60F_{254}$ (0.2 mm) precoated aluminum foils. Preparative TLC: plates ($20 \times 20 \times 0.2$ cm^3) precoated with silica gel 60 (E. Merck). Medium-pressure chromatography (MPLC):[36] E. Merck silica gel 60 (40−63 μm).

Instrumentation. Melting points (mp) were determined with a hot stage apparatus (Thermovar, C. Reichert AG, Vienna) and are uncorrected. UV/vis spectra (λ_{max} in nm, log ϵ in parentheses) were recorded on a Hewlett-Packard-8452A diode-array spectrophotometer. Specific optical rotations ($[\alpha]^{20}_D$) were measured on a Perkin-Elmer-241-MC polarimeter and CD spectra on a Jobin-Yvon-Auto-Dichrograph Mark V. Wavelengths (λ) and band amplitudes ($\Delta\epsilon_{max}$) are quoted in nm and L mol^{-1} cm^{-1}, respectively. Quantum yields of fluorescence (Φ) were measured relative to rhodamine 6G (Φ 0.88 in EtOH), as standard,[37] on a Perkin-Elmer-MPF-4 fluorescence spectrophotometer. NMR: Varian Gemini 200 (^{1}H, 200.00; ^{13}C, 50.30 MHz), Bruker Avance DRX500 (^{1}H, 500.13; ^{19}F, 470.52; ^{13}C, 125.76 MHz), or Bruker-AM 360 (^{1}H, 360.14; ^{13}C, 90.57 MHz) equipped with a data system Aspect 3000; ^{1}H and ^{13}C chemical shifts (δ) are given in ppm relative to Me_4Si as internal standard; ^{19}F chemical shifts are relative to BF_3 etherate as external standard. *J* values are in Hz; assignments are based on homonuclear COSY-45, ^{1}H{^{1}H} NOE difference correlations, and/or chemical shifts; ^{13}C signal multiplicities were determined by attached proton test (APT) experiments. FAB mass spectra (FAB-MS): Vacuum Generators Micromass 7070 E instrument equipped with a data system DS 11-250; FAB ionization (at 6 kV) in 3-nitrobenzyl alcohol (NBA) or glycerol/thioglycerol (G/TG) with Ar at 8 kV; *m/z* and relative intensities (%) are in parentheses.

***tert*-Butyl (−)-(*S*)-5-[(4-Ethyl-2,5-dihydro-3-methyl-5-oxo-1*H*-pyrrol-2-yl)methyl]-4-methyl-1*H*-pyrrole-2-carboxylate (1b).** The

(33) Falk, H.; Hofer, O.; Lehner, H. *Monatsh. Chem.* **1974**, *105*, 169.
(34) Schellman, J. A. *J. Chem. Phys.* **1966**, *44*, 55; *Acc. Chem. Res.* **1968**, *1*, 144.
(35) Klyne, W.; Kirk, D. N. *Tetrahedron Lett.* **1973**, 1483−1486.
(36) Loibner, H.; Seidl, G. *Chromatographia* **1979**, *12*, 600.
(37) Olmsted, J. *J. Phys Chem.* **1979**, *83*, 2582.

corresponding optically active (ee 98%) carboxylic acid (**1a**)[6] (25 mg) was suspended under Ar in dry CH_2Cl_2 (2 mL) containing *tert*-butyl acetate (2.0 mL) before 50 μL of freshly distilled BF_3 etherate was added under Ar. After 4 h of stirring at room temperature, the mixture was diluted with 20 mL of CH_2Cl_2 and shaken with H_2O (3 × 20 mL). The organic layer was separated and dried (Na_2SO_4), and the solvent was evaporated to yield 18.4 mg (61%) of **1b**, which was crystallized from *n*-hexane/ethyl acetate. Mp: 218−219 °C. $[\alpha]^{20}_D = -89.1$ (*c* = 19.1 mg/100 mL, MeOH). Ee: 98% (determined by ^{1}H-NMR in (−)-(*R*)-1-(9-anthryl)-2,2,2-trifluoroethanol as chiral solvating agent[38]). UV/vis (MeOH, 1.9×10^{-5} M): 282 (4.58). CD (1.9×10^{-5} M in MeOH): 282 (−7.12). ^{1}H-NMR (500.13 MHz, CD_2Cl_2): 9.54 (s, br, H-N(11)), 6.54 (d, *J* = 2.5, H-C(8)), 6.42 (br *s*, H-N(10)) 4.06 (dd, *J* = 3.8, 9.4, H-C(4)), 3.08 (dd, *J* = 4.1, 14.6, (*pro-S*)H-C(5)), 2.49 (dd, *J* = 9.4, 14.5, (*pro-R*)H-C(5)), 2.20 (q, *J* = 7.6, *CH*$_2$-C(2)), 2.03 (s, *Me*-C(7)), 1.96 (s, *Me*-C(3)), 1.49 (s, *Me*$_3$C(9^3)), 0.99 (t, *J* = 7.6, *Me*-CH_2-C(2)). ^{13}C-NMR (125.76 MHz, CD_2Cl_2): 174.4 (s, OC(1)), 161.0 (s, OC(9^1)), 151.7 (s, C(3)), 134.7 (s, C(2)), 129.9 (s, C(6)), 122.7 (s, C(9)), 118.1 (s, C(7)), 116.52 (*d*, C(8)), 80.6 (s, C(9^2)), 59.9 (*d*, C(4)), 29.9 (t, C(5)), 28.5 (q, (H$_3$*C*)$_3$C), 16.9 (t, C(2^1)), 13.2 (q, C(2^2)), 12.2 (q, C(7^1)), 11.1 (q, C(3^1)). FAB-MS (G/TG): 319 (10, $[M + H]^+$), 263 (80), 245 (50), 215 (9), 194 (22), 138 (100), 120 (27), 91 (37). Anal. Calcd for $C_{18}H_{26}N_2O_3$: C, 67.90; H, 8.23; N, 8.80. Found: C, 67.63; H, 8.34; N, 8.74.

Difluoro[(−)-(4*S*,16*S*)-2,18-Diethyl-1,4,5,15,16,19,21,24-octahydro-3,7,13,17-tetramethyl-1,19-dioxo-22*H*-bilinato(1−)-*N*^{22},*N*^{23}]boron (5). A solution of the urobilin hydrochloride **3**[6] (22 mg, 0.045 mmol) in dry CH_2Cl_2 (50 mL) was cooled under Ar to −5 °C before 0.1 mL of *N*,*N*-diisopropylethylamine was added, whereby the color of the solution changed from red to yellow. After 15 min of stirring, freshly distilled BF_3 etherate (1.0 mL) was added dropwise, during a 5 min period, in order to avoid a rise of the temperature due to the exothermic reaction which takes place. After 10 min, the same portions of *N*,*N*-diisopropylethylamine and BF_3 etherate were added likewise, and thereafter, the pink-red strongly fluorescent mixture was stirred for 90 min at −5 °C before it was diluted with CH_2Cl_2 (50 mL) and washed with H_2O (4 × 50 mL). The organic layer was dried ($MgSO_4$), and the solvent was evaporated under reduced pressure. From the residue, pink-violet and orange-brown major bands were separated by preparative TLC (five plates, 20 × 20 × 0.2 cm^3, Merck Kieselgel 60 HF, CH_2Cl_2/MeOH = 95:5); the orange-brown band consisted of starting material, which after being eluted from the silica gel with MeOH was treated again with *N*,*N*-diisopropylethylamine (0.2 mL) and BF_3 etherate (2.0 mL) and worked up as before. The main and subsidiary samples eluted with MeOH from the pink-violet band were combined and subjected again to preparative TLC (two plates, as before) to obtain 6.2 mg (28%) of pure **5**. TLC (CH_2Cl_2/MeOH = 97:3): R_f 0.29. Mp: 250 °C (dec). UV/vis (DMF, 5.4×10^{-5} M): 366 (3.44), 518 (sh., 3.90), 544 (4.26). UV/vis (CH_2Cl_2, 9.7×10^{-5} M): 366 (3.62), 516 (sh., 4.16), 546 (4.36). Emission spectrum (CH_2Cl_2): λ_{max} (exc.) 366; λ_{max} (em.) 552. Φ: 0.57. $[\alpha]^{20}_D = -2940 \pm 15$ (*c* = 4.8 mg/100 mL, CH_2Cl_2). CD (3.65×10^{-5} M, DMF, 20 °C): 546 (−7.98). Temperature dependence (°C): −10.9 (−20), −10.3 (−10), −9.43 (0); −8.7 (+10), −7.61 (+30), −7.25 (+40), −7.07 (+50). CD (5.18×10^{-5} M, CH_2Cl_2, 20 °C): 545 (−9.70). Temperature dependence (°C): −11.4 (−20), −10.8 (−10), −10.2 (0); −9.83 (+10), −9.31 (+30), −8.80 (+40). ^{1}H-NMR (360.14 MHz): Tables 1 and 2. ^{13}C-NMR (125.76 MHz, CD_2Cl_2): 174.25 (s, 2 × CO), 156.66 (s, C(6), C(14)),[39] 152.10 (s, C(3), C(17)),[39] 134.45 (s, C(2), C(18)),[39] 134.38 (s, C(9), C(11)),[39] 130.08 (d, C(8), C(12)),[40] 129.79 (s, C(7), C(13)),[39] 126.87 (d, C(10)),[40] 59.97 (d, C(4), C(16)),[40] 31.27 (t, C(5), C(15)),[40] 17.02 (t, Me-*C*H$_2$-C(2), Me-*C*H$_2$-C(18)),[40] 13.29 (q, *Me*-CH$_2$-C(2), *Me*-CH$_2$-C(18)),[40] 12.21 (q, *Me*-C(3), *Me*-C(17)),[40] 11.76 (q, *Me*-C(7), *Me*-C(13)).[40] ^{19}F-NMR: 10.87 (in DMF-d_7) or 12.41 (in CD_2Cl_2) (both q, $^1J(^{19}F-^{11}B) = 33.7$). FAB-MS (NBA): 517 (10, $[M + Na]^+$), 495 (36, $[M + H]^+$), 455 (6), 370 (14), 350 (14), 331 (16), 247 (20), 227 (100), 199 (4), 176 (5). HR-FAB-MS (G/TG): 495.2743 ($[C_{27}H_{34}BF_2N_4O_2]^+$; calcd 495.2742).

Difluoro[(−)-(4*R*,16*R*)-1,4,5,15,16,19,21,24-octahydro-4,7,8,12,13,16-hexamethyl-1,19-dioxo-22*H*-bilinato(1−)-*N*^{22},*N*^{23}]boron (6 and 7). A solution of **2**[7] (46 mg, 0.15 mmol) in CF_3CO_2H (5 mL) was stirred under Ar at room temperature for 15 min before a solution of the corresponding 9-aldehyde[7] (36 mg, 0.16 mmol) in CF_3CO_2H (5 mL) was added at once. After 15 min, the mixture was cooled in an ice bath, MeOH (1 mL) was added, and stirring was continued for 1 h at room temperature. Then, the solvent was evaporated to dryness, the residue was dissolved in CH_2Cl_2, and the stirred solution was cooled to 0 °C before *N*,*N*-diisopropylethylamine (0.5 mL) was added. After 5 min, freshly distilled BF_3 etherate (1.0 mL) was added dropwise within a period of 5 min. After 10 min, the same quantities of *N*,*N*-diisopropylethylamine and BF_3 etherate were added, as previously described, and the mixture was stirred for 30 min at 0 °C, before it was diluted with 50 mL of CH_2Cl_2. The solution was shaken with aqueous $NaHCO_3$ and H_2O, then dried (Na_2SO_4), and finally, the solvent was evaporated. The residue was subjected to MPLC (CH_2Cl_2/MeOH = 9:1) to yield 44 mg (63%) of the BF_2 chelate of **4**, as a dark-red solid, which was recrystallized from CH_2Cl_2/*n*-hexane: mp 240 °C (dec). UV/vis (DMF, 1.14×10^{-5} M): 388 (3.89), 502 (sh., 4.42), 536 (4.84). UV/vis (CH_2Cl_2, 1.2×10^{-5} M): 388 (3.92), 504 (sh., 4.34), 538 (4.84). Emission spectrum (CH_2Cl_2): λ_{max} (exc.) 366; λ_{max} (em.) 546. Φ: 0.48. $[\alpha]^{20}_D = -3900$ (*c* = 5.311 mg/100 mL, DMF). $[\alpha]^{20}_D = +9700$ (*c* = 5.614 mg/100 mL, CH_2Cl_2). CD (1.46×10^{-5} M, DMF, 20 °C): 535 (−29.5). Temperature dependence (°C): −48.1 (−20), −39.5 (−10), −35.4 (0); −32.2 (+10), −19.5 (+30), −17.7 (+40), −12.7 (+50). CD (1.32×10^{-5} M, CH_2Cl_2, 20 °C): 538 (+67.2). Temperature dependence (°C): + 82.1 (−20), + 79.2 (−10), + 76.0 (0); +72.1 (+10), + 58.1 (+30), +49.9 (+40). ^{1}H-NMR (360.14 MHz): Tables 3 and 4. ^{13}C-NMR (90.57 MHz, in CD_2Cl_2): 172.70 (s, 2 × CO); 154.98 (d, C(3), C(17)); 153.41, 139.96, 133.67, 126.69 (4 × s, C(6), C(7), C(8), and C(9)); 126.21 (d, C(2), C(18)); 65.03 (s, C(4), C(16)); 35.62 (t, C(5), C(15)); 26.94 (q, *Me*-C(4), *Me*-C(16)); 10.82 (q, *Me*-C(8), *Me*-C(12)); 10.34 (q, *Me*-C(7), *Me*-C(13)).^{19}F-NMR: 16.44 (in DMF-d_7) or 18.40 (in CD_2Cl_2) (both q, $^1J(^{19}F-^{11}B) = 33.7$). FAB-MS (NBA): 489 (12, $[M + Na]^+$), 467 (23, $[M + H]^+$), 427 (13), 370 (16), 350 (14), 331 (13), 255 (100). HR-FAB-MS (NBA): 467.2426 ($[C_{25}H_{30}BF_2N_4O_2]^+$; calcd 467.2429).

Acknowledgment. Financial support of this work by the Swiss National Foundation (Project No. 20-42420.94) is gratefully acknowledged. We are greatly indebted to Dr. P. G. Scherer (Spectrospin AG, CH-8117 Fällanden) for inverse gated ^{19}F GARP decoupling measurements carried out with compound **7**. We thank Prof. Dr. T. A. Jenny for valuable suggestions and his assistance in interpreting the spectra, as well as Prof. W. Hug (Institut für Physikalische Chemie der Universität Fribourg) for helpful discussions. Elemental analyses were carried out at Ciba Geigy AG, Forschungszentrum, CH-1723 Marly.

Supporting Information Available: ^{1}H-NMR and ^{19}F-NMR **5**−**7** and ^{13}C-NMR and FAB-MS spectra for **5** and **7** (12 pages). See any current masthead page for ordering and Internet access instructions.

JA961883Q

(38) Pirkle, W. H.; Sikkenga, D. L.; Pavlin, M. S. *J. Org. Chem.* **1977**, *42*, 384.

(39) Assignments made in a 125.76 MHz COLOC spectrum.

(40) Assignments made in a 125.76 MHz HETCOR spectrum.